# Theoretical modeling of the kinetics of fibrilar aggregation of bovine β-lactoglobulin at *p*H 2

Luben N. Arnaudov[a] and Renko de Vries
*Laboratory of Physical Chemistry and Colloid Science, Wageningen University, Dreijenplein 6, 6700 EK Wageningen, The Netherlands and Food Physics Group, Wageningen University, Bomenweg 2, 6703 HD Wageningen, The Netherlands*

(Received 29 September 2006; accepted 13 February 2007; published online 12 April 2007)

The authors propose a kinetic model for the heat-induced fibrilar aggregation of bovine β-lactoglobulin at *p*H 2.0. The model involves a nucleation step and a simple addition reaction for the growth of the fibrils, as well as a side reaction leading to the irreversible denaturation and inactivation of a part of the protein molecules. For the early stages of the aggregation reaction, the authors obtain an analytical solution of the model. In agreement with their experimental results, the model predicts a critical protein concentration below where almost no fibrils are formed. The model agrees well with their experimental data from *in situ* light scattering. By fitting the experimental data with the model, the authors obtain the ionic strength dependent kinetic rate constants for β-lactoglobulin fibrilar aggregation and the size of the critical nucleus. © *2007 American Institute of Physics*. [DOI: 10.1063/1.2717159]

## INTRODUCTION

From a previous study[1] we know that the fibrilar aggregation of (β−lg) at *p*H 2.0 and low ionic strength induced by heating at 80 °C is a complex, multistep process. The fibril formation is partially reversible upon cooling of the solution. We have also shown by *in situ* light scattering[2] that there is an apparent critical concentration for fibril formation for β−lg solutions at *p*H 2.0 and various ionic strengths, due to the competition between two processes (i) inactivation of the protein molecules by irreversible denaturation and (ii) fibril formation from partially unfolded protein molecules. The critical concentration for fibril formation was found to be a sharply decreasing function of the ionic strength.[2] Here we focus on kinetic modeling with the intent of elucidating the ionic strength dependence of the aggregation mechanism.

Various models are available for the kinetics of protein aggregation,[3] but only a few apply to irreversible fibril formation.[4–9] The latter kinetic models are mostly simplified to a degree where the whole process is described by a single differential equation of the form

$$\frac{dc}{dt} = -k_n c^n, \tag{1}$$

where $c$ is the protein monomer concentration, $k_n$ is the rate constant, and $n$ is the order of the reaction. The order most commonly reported in the literature is between 1 and 2.[10] However, protein aggregation is a complex process usually involving two or more consecutive steps. The description of the kinetics of such a process by Eq. (1) amounts to the replacing of several simultaneous or consecutive reactions by a single, rate-determining step. In case of a nucleation and growth type of aggregation, the rate-determining step can be the formation of the nucleus.[11]

Furthermore, it is well known that when one deals with a (pseudo)equilibrium process the route from the initial to the final state is irrelevant. In the case of irreversible or partially reversible processes, however, the detailed path between the initial and the final state of the system is of great importance.[12] Our system seems to be in that category.[1,2] Last, but not the least, for the kinetics of fibril formation from β−lg at *p*H 2.0 and different ionic strengths no model has been elaborated.

Here we develop a detailed model for the heat-induced fibril formation of β−lg at *p*H 2.0 and use it to describe our experimental data obtained using *in situ* light scattering.[2] The modeling of the process of aggregation offers a variety of possibilities to analyze the experimental kinetic data.[11] The model allows us to obtain an expression for the apparent critical concentration for fibril formation from β−lg in terms of ionic strength dependent rate constants; values for the rate constants are extracted from our data by fitting to the model.

## MATERIALS AND METHODS

### Materials

Bovine β-lactoglobulin (β−lg.) was obtained from SIGMA (Ref. L0130, lot 21K7079). It is a mixture of genetic variants A and B and is used throughout all experiments. All solutions were prepared with de-ionized water (Barnstead) and contained 200 ppm $NaN_3$ to prevent bacterial growth. The *p*H was adjusted by addition of small amounts of 1*M* HCl (Merck, Darmstadt, Germany). The ionic strength of the solutions was adjusted by addition of NaCl (Merck). Prior to use a concentrated solution of β−lg at *p*H 2.0 was extensively dialyzed against the solvent. After dialysis, the β−lg solutions were centrifuged for 3 h at 45 000 g using a Beckman Avanti J-25I high performance centrifuge and subse-

[a]Author to whom correspondence should be addressed. Tel.: +31 (0)317 482194; Fax: +31 (0)317 483777. Electronic mail: luben.arnaudov@wur.nl

 

quently filtered through 0.45 $\mu$m low protein adsorbing syringe filters (Sterile Acrodisk, Gelman Sciences) into the glass tubes in which the experiments were subsequently carried out. The solutions used in all the experiments were prepared by dilution from the dialyzed ones. Care was taken to minimize dust. Glassware was cleaned with chromic acid, rinsed repeatedly with de-ionized water, and dried in a clean environment. The solutions for the light scattering experiments were filtered through 0.1 $\mu$m syringe filters (Sterile Acrodisk, Gelman Sciences) directly into the clean glass tubes prior to the experiments. The protein concentrations were determined by spectrophotometry at $\lambda = 278$ nm, using an extinction coefficient of 0.83 L $g^{-1}$ $cm^{-1}$.

### Light scattering (LS)

Static and dynamic light scattering data were obtained at a scattering angle of 90° using an ALV/SLS/DLS-5000 light scattering apparatus (Langen, Germany), equipped with an argon ion laser (LEXEL, Palo Alto, CA) emitting vertically polarized light at a wavelength of 514.5 nm. The intensity of the scattered light was calibrated against scattered light from pure toluene measured before each series of experiments at 25 °C. The scattering from the solvent was accounted for by subtracting the corresponding intensity from that of the protein sample. Before the start of the heating, the absence of other than monomeric protein in the sample tubes was established by dynamic light scattering at 25 °C for each sample. The aggregation process was then followed *in situ* by directly inserting the sample in the preheated sample holder of the light scattering (LS) setup which was at 80 °C, keeping it there for a period of time ranging from 1 to 24 h, while collecting scattering data, and subsequently quenching the sample in ice-cold water.

## THEORETICAL BACKGROUND

### Kinetics of protein aggregation

To derive a kinetic model for the heat-induced aggregation of $\beta$−lg at *p*H 2.0 we follow Ferrone.[11] Since we already know that at *p*H 2.0 and low ionic strength $\beta$−lg undergoes at least two simultaneous reactions, one of which is the actual linear aggregation and the other one is the irreversible denaturation of the protein molecule to an inactive species,[1,2] we need a kinetic model with a side reaction accounting for latter step that we will further call *inactivation*. Because the model aims at describing experimental data obtained from an *in situ* study we need not take into account the partial reversibility of the fibril formation upon cooling.[1] The simplest general model for the aggregation of $\beta$−lg at *p*H 2.0 can be presented by a side reaction (inactivation of protein molecules), a nucleation step, and a simple addition reaction,[3,11]

$$
\begin{aligned}
&A_1 \underset{k_-^u}{\overset{k_+^u}{\leftrightarrow}} A_1^u \quad \text{(step 1)},\\
&n^* A_1 \underset{k_-^*}{\overset{k_+^*}{\leftrightarrow}} A_{n^*} \quad \text{(step 2)},\\
&A_1 + A_i \underset{k_-^i}{\overset{k_+^i}{\leftrightarrow}} A_{i+1}, i > n^* \quad \text{(step 3)},
\end{aligned} \tag{2}
$$

where $A_1$ represents the monomer species, $A_1^u$ the inactivated monomer species, with $k_+^u$ being the forward rate and $k_-^u$ the backward rate of inactivation, $n^*$ is the size of the critical nucleus, $k_+^*$ and $k_-^*$ are the respective rate constants for the formation and disassembly of the nucleus, $A_i$ represents the $i$-mers, $A_{i+1}$ the $i+1$-mers, and $k_+^i$, and $k_-^i$ are the respective forward and backward rate constants for the $i$th reaction. This scheme is analogous to schemes encountered in polymerization kinetics; steps 2 and 3 are analogous to initiation, and propagation and step 1 would be an initiator degradation reaction.[13] In the real process of aggregation all of the above reactions are preceded by an activation step of the protein monomers which amounts to a partial unfolding of the protein molecules, i.e., to denaturation. Because we have previous evidence from proton NMR spectroscopy[1] that $\beta$−lg molecules at *p*H 2.0 unfold as soon as the temperature is increased above 70 °C, and because we observe the aggregation to start immediately after the necessary temperature is reached, and the time for which we collect data is of the order of tens of seconds, we can consider the process of activation to be much faster than all the other reactions, and therefore we do not take it into consideration. The same holds for the equilibrium between monomers and dimers.

According to the model (2) part of the active protein molecules are transformed into an inactive state, in which they cannot form aggregates anymore. Therefore, at every moment in our solution, we can write the monomeric protein concentration in the form

$$c_1(t) = c_1^a(t) + c_1^b(t), \tag{3}$$

where $c_1^a(t)$ is the momentary concentration of the active protein monomers that can form aggregates, and $c_1^b(t)$ is the concentration of the inactivated monomeric protein that cannot form aggregates anymore. Then from the first reaction in the kinetic model (2) we have

$$\frac{dc_1^b}{dt} = k_+^u c_1^a(t) - k_-^u c_1^b(t). \tag{4}$$

A common approach to the linear aggregation of proteins is to assume that all forward rates $k_+^i$ [see Eq. (2)] are equal to $k_+$ and all backward rates $k_-^i$ are equal to $k_-$. Then, the model (2) can be represented, together with Eq. (4), by the following system of ordinary differential equations

$$\frac{dc_i}{dt} = k_+ c_{i-1} c_1^a - k_- c_i - k_+ c_i c_1^a + k_- c_{i+1}, \quad i > n^*, \tag{5}$$

$$\frac{dc_{n^*}}{dt} = -k_+ c_{n^*} c_1^a + k_- c_{n^*+1} + k_+^* (c_1^a)^{n^*} - k_- c_{n^*}, \tag{6}$$

where Eq. (5) represents the change in the number concentration of $i$-mers, and Eq. (6) represents the change in the number concentration of nuclei. Summing Eq. (5) for all $i$'s greater than $n^*$ and taking into account Eq. (6) gives an equation for the total concentration of polymers $c_p(t)$

$$\frac{dc_p}{dt} = \frac{d\left(\sum_{i=n^*}^{\infty} c_i\right)}{dt} = k_+^* (c_1^a)^{n^*} - k_- c_{n^*}. \tag{7}$$

Multiplying Eq. (5) by $i$ and Eq. (6) by $n^*$ and summing for all $i$'s greater than $n^*$ gives an equation for the total concentration of monomers participating in polymers $c_h(t) = c_0 - c_1(t)$, with $c_0$ being the initial monomer concentration,

$$\frac{dc_h(t)}{dt} = \frac{d\left(\sum_{i=n^*}^{\infty} i c_i\right)}{dt} = -\frac{dc_1(t)}{dt}$$

$$\frac{dc_h(t)}{dt} = (k_+ c_1^a - k_-) c_p(t) + n^* \frac{dc_p(t)}{dt} + k_- c_{n^*}. \tag{8}$$

Because the intensity of scattered light is proportional to the second moment of the polymer (aggregate) distribution (see the next section), we need an equation for that quantity which we obtain by multiplying Eq. (5) by $i^2$ and summing for all $i$'s greater than $n^*$,

$$\frac{dc_d(t)}{dt} = \frac{d\left(\sum_{i=n^*}^{\infty} i^2 c_i\right)}{dt}$$

$$\frac{dc_d(t)}{dt} = 2(k_+ c_1^a - k_-) c_h(t) + (k_+ c_1^a + k_-) c_p(t) + (n^*)^2 \frac{dc_p(t)}{dt} + (2n^* - 1) k_- c_{n^*}. \tag{9}$$

If one ignores the back rates in Eqs. (4) and (7)–(9), which is justified for an irreversible reaction, then the system has an analytical solution.[3] A simple way to obtain an analytical solution of the system (4) and (7)–(9) is the approach of Ferrone,[11] in which the equations are linearized, i.e., to make a series expansion of the right hand side of the equations with respect to the concentration and keep the linear terms. One should note that in Eq. (8) $c_p(t)$ is already small, as well as $c_h(t)$ in Eq. (9). For more details about the linearization procedure, one may look in Ferrone.[11] Ignoring the back rates and expanding Eqs. (4) and (7)–(9) in series with respect to concentration and keeping only the linear terms we obtain the set

$$\frac{dc_1^b(t)}{dt} = k_+^u c_0 - k_+^u [c_1^b(t) + c_h(t)], \tag{10}$$

$$\frac{dc_p(t)}{dt} = k_+^* c_0^{n^*} - k_+^* n^* c_0^{n^*-1} [c_1^b(t) + c_h(t)], \tag{11}$$

$$\frac{dc_h(t)}{dt} = n^* \frac{dc_p(t)}{dt} + k_+ c_0 c_p(t), \tag{12}$$

$$\frac{dc_d(t)}{dt} = (n^*)^2 \frac{dc_p(t)}{dt} + 2k_+ c_0 c_h(t) + k_+ c_0 c_p(t), \tag{13}$$

which is to be solved with the initial conditions,

$$c_1^b(0) = 0, \quad c_p(0) = 0, \quad c_h(0) = 0, \quad c_d(0) = 0. \tag{14}$$

The set (10)–(14) has analytical solution details about which are given in the Appendix. The sought second moment of the fibril distribution has the analytical form

$$\frac{c_d(\tau)}{c_0} = f_1[1 - \exp(-\beta\tau)\cosh(\beta\tau\sqrt{1-\chi})] + f_2 \exp(-\beta\tau) \frac{\sinh(\beta\tau\sqrt{1-\chi})}{\sqrt{1-\chi}} - f_3\tau + f_4\tau^2, \tag{15a}$$

$$\frac{c_d(\tau)}{c_0} = f_1[1 - \exp(-\beta\tau)\cos(\beta\tau\sqrt{\chi-1})] + f_2 \exp(-\beta\tau) \frac{\sin(\beta\tau\sqrt{\chi-1})}{\sqrt{\chi-1}} - f_3\tau + f_4\tau^2, \tag{15b}$$

where $\tau = k_+^u t$, $\beta = \frac{1}{2}[a(n^*)^2 + 1]$, $\chi = 4abn^*/[a(n^*)^2 + 1]^2$, and $a$, $b$, $f_1$, $f_2$, $f_3$, and $f_4$, are factors given in the Appendix. The functional form of the solution depends on the sign of $1-\chi$. It is different for positive [Eq. (15a)] and negative [Eq. (15b)] values of $1-\chi$ and for $\chi = 1$ the solution is degenerate. Since the change in the functional form of the solution occurs when $\chi$ passes through 1, we can use this fact and determine a kinetic "critical" concentration by defining $c_0 = c_{cr}$ when $\chi = 1$. Then having in mind that $a(n^*)^2 \ll 1$ at protein concentrations not much larger than the critical one, we get the expression

$$c_{cr} \approx \left[\frac{(k_+^u)^2}{4n^* k_+ k_+^*}\right]^{1/n^*}. \tag{16}$$

If one has the value of the critical concentration from an independent source, the parameter $\chi$ can be calculated by the expression

$$\chi \approx \left(\frac{c_0}{c_{cr}}\right)^{n^*}. \tag{17}$$

Thus, effectively, the number of free parameters in Eq. (15) is decreased. One should note that the solution (15), i.e., (A7)–(A10), is valid only for the early stages of the aggregation where the linearization (10)–(14) is valid. Therefore, it is also justifiable for data fitting purposes, instead of Eq. (15), to use series expansion with respect to time and keep only the first two terms. Doing so one finds

$$c_d(t) = c_0 A_1 t + c_0 B_1 \frac{t^2}{2} + O(t^3), \tag{18}$$

where

$$A_1 = (n^*)^2 k_+^* c_0^{n^*-1}, \tag{19}$$

$$B_1 = (2n^* + 1) k_+^* k_+ c_0^{n^*} - A_1(n^* k_+^u + A_1). \tag{20}$$

For protein concentrations exceeding the critical one the second term on the right hand side of Eq. (20) is much smaller than the first one, so we can simplify it to

$$B_1 \approx (2n^* + 1)k_+^* k_+ c_0^{n^*}. \tag{21}$$

One can see from Eqs. (19)–(21) that $A_1$ and $B_1$ should depend on the protein concentration $c_0$ and can be used at sufficiently high protein concentrations (above the critical one) to determine a number of kinetic parameters. From Eq. (21), it can be seen that above the critical concentration $B_1$ is a straight line in a log-log plot as a function of the concentration $c_0$ with the slope being the size $n^*$ of the critical nucleus in the model (2). Knowing the size of the critical nucleus one can use the concentration dependence of the parameters $A_1$ and $B_1$ and determine the values of the kinetic parameters $k_+^*$ and $k_+$, respectively. Consequently, the values of the parameters $n^*$, $k_+^*$, $k_+$, and the value for the critical concentration $c_{cr}$, can be substituted in Eq. (16), and the value of the rate of inactivation $k_+^u$ can be obtained.

At low protein concentrations, the parameter $B_1$ in Eq. (18) can become very small or even negative because of the second term on the right hand side of Eq. (20). In those cases, it is not justified to use the quadratic expansion (18) since a linear one would suffice and we would essentially obtain less information from the numerical fits of the experimental data. Moreover, at low protein concentrations the solutions scatter less, which influences the accuracy of the experimental data and, therefore, the accuracy of the obtained fitting parameters. In short, experimental data around the critical concentration and above it are most useful.

### Static light scattering

Static light scattering (SLS) is a very useful experimental technique because under certain assumptions the scattered intensity can be related to the second mathematical moment of the distribution of scattering objects. Below, we discuss the background of SLS and the way to relate the concentration of scattering species to the scattered intensity.

For the initial times of the aggregation process when the aggregate size is still small and the monomers and polymers do not interact strongly, the intensity of the scattered light can be written as[14]

$$R_\theta(q,t) = \frac{KM_1^2}{N_A}\sum_{i=1}^{\infty} i^2 c_i(t), \tag{22}$$

where $R_\theta(q,t)$ is the Rayleigh ratio, $q=(4\pi n/\lambda)\sin(\theta/2)$ is the wave vector, $\theta$ is the scattering angle, $\lambda$ is the wave length of the incident beam, $c_i$ is the number concentration of species $i$, $M_1$ is the molecular weight of the monomers in g/mol. $K$ is an optical constant, and $N_A$ is Avogadro's number. For measurement purposes, the Rayleigh ratio has to be calibrated against a scattering standard such as liquid toluene. One then has

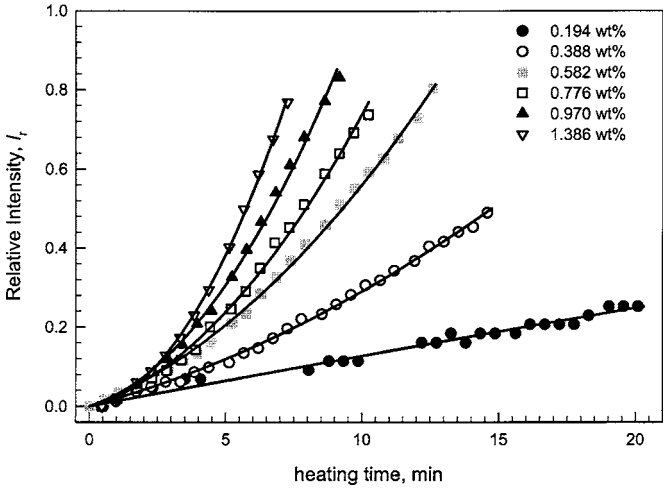


FIG. 1. Relative scattered intensity of $\beta$-lg solutions at different concentrations at $p$H 2.0 and ionic strength I=70 mM as a function of heating time at 80 °C, as determined by LS. The solid lines through the data points are obtained by best fits to the experimental data.

$$R_\theta(q) = \frac{I(q) - I_{sol}(q)}{I_{tol}(90^\circ)}\left(\frac{n_{tol}}{n_s}\right)^2 R_{tol}, \tag{23}$$

where $n_{tol}$ is the refractive index of toluene and $R_{tol}$ is the Rayleigh ratio of toluene which is taken to be $3.2 \times 10^{-5}\text{cm}^{-1}$ for 514.5 nm. In that case if we define a relative intensity of the scattered light, we obtain

$$I_r(t) = \frac{I(t) - I_{sol}}{I(0) - I_{sol}} - 1 = \frac{R_\theta(t)}{R_\theta(0)} - 1 = \frac{\sum_{i=1}^{\infty} i^2 c_i(t)}{c_0} - 1 \approx \frac{c_d(t)}{c_0}. \tag{24}$$

In other words, the relative intensity of the scattered light is proportional to the second moment of the fibril distribution in the initial stage of the aggregation when $qR<1$ and the series expansion, Eq. (18), holds. We have shown this to be the case for our experimental system by using dynamic light scattering in a previous study.[2] Thus, we can use the expansion (18) and fit the relative scattered intensity (24) measured during the aggregation process, so obtaining the dependence of the kinetic parameters on protein concentration and ionic strength.

## RESULTS AND DISCUSSION

We study the kinetics of protein aggregation with the help of the scattered intensity from the solution during the process of aggregation.[2] Figure 1 shows an example of the relative scattered intensity from a $\beta$-lg solution with different concentrations at 70 mM ionic strength. The lines through the experimental points are obtained by a linear least squares fit of the data with the equation

$$I_r(t) = At + Bt^2, \tag{25}$$

where $A=A_1$ and $B=B_1/2$ with $A_1$ defined by Eq. (19), and $B_1$ defined by Eq. (21). Our model predicts values of $A$ and $B$ that depend on the initial protein concentration through Eqs. (19) and (21).

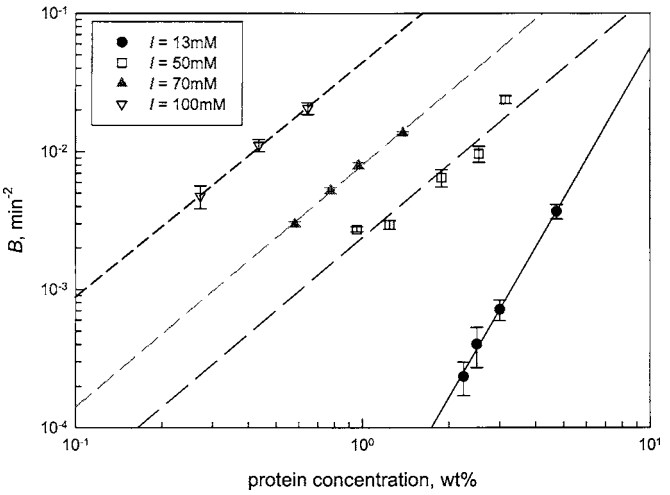


FIG. 2. Kinetic coefficients $B$ for $\beta$-lg solutions at different ionic strengths plotted as a function of protein concentration obtained from numerical fit to the experimental data with the kinetic model.

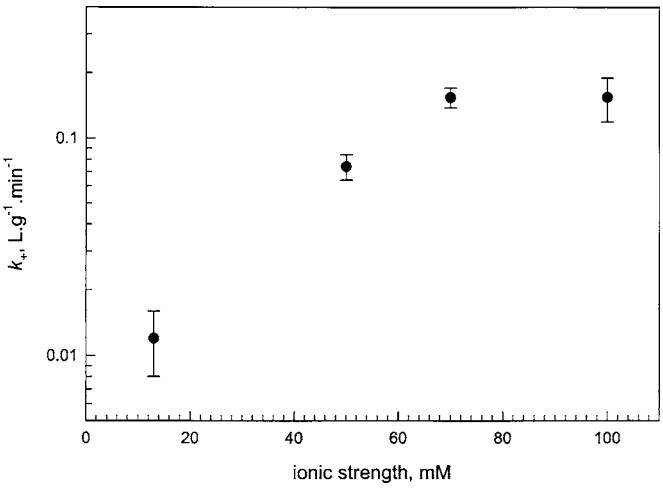


FIG. 3. Rate of fibril elongation as a function of the ionic strength of the studied solutions estimated from numerical fit to the experimental data with the kinetic model proposed by us.

Figure 2 shows the values of the coefficients $B$ above the critical concentration plotted versus the protein concentration in a log-log plot for all the studied ionic strengths. From the dependence of the coefficient $B$ on the initial protein concentration [Eq. (21)] it follows that the slope of the dependence of $\log B$ on $\log c$ must be $d \log B / d \log c_0 = n^*$, so by the slope of the $\log B(\log c)$ dependence above the critical concentration we can determine the size of the nucleus for the aggregate formation.[3,11] One can see that the slopes of the dependencies for all ionic strengths higher than 13 mM are virtually the same. The sizes of the nuclei, which we obtain, are $3.6 \pm 0.1$ for 13 mM ionic strength, $2.0 \pm 0.2$ for 50 mM ionic strength, $1.8 \pm 0.1$ for 70 mM ionic strength, and $1.7 \pm 0.1$ for 100 mM ionic strength. From what we know, until now it appears that the reaction mechanism of the fibrilar aggregation of $\beta$-lg at $p$H 2.0 and different ionic strengths is similar for all ionic strengths and proceeds through two distinct but simultaneous processes—formation of linear aggregates and inactivation of the protein. There is a qualitative difference in the size of the nucleus for 13 mM ionic strength and the other ionic strengths. The increase of the ionic strength decreases the effect of the electrostatic repulsion between the protein molecules and thus accelerates the aggregation. This can be discussed in terms of a balance between the nucleation and elongation reactions from one side and the protein inactivation from the other one. As nucleation and elongation are processes involving two or more molecules, they are strongly affected by the electrostatic interaction, whereas the effect of the ionic strength on the rate of protein inactivation, which presumably is a monomolecular reaction, should be less pronounced.

A possible reason for the difference between the sizes of the nuclei at 13 mM ionic strength and the higher ionic strengths could be the greater importance of the mutual orientation of the molecules at the lowest ionic strength: at 13 mM the electrostatic screening length is still of the order of the size of the protein molecule. Since presumably, the positive charges of the $\beta$-lg molecule are distributed unevenly the electric field in close vicinity of the protein molecule is asymmetrical. We can then speculate that maybe four $\beta$-lg molecules are necessary to symmetrize the electric field near the nucleus and thus make further addition of molecules easier. For higher ionic strengths the screening length becomes smaller than the size of the protein molecule and the formation of a dimer becomes the rate limiting step in the aggregation.

Once we have the values for the sizes of the critical nuclei and the values of the critical concentration for different ionic strengths,[2] we can use Eqs. (16), (19), and (21) to estimate the values of the rest of the kinetic parameters, the rate of nucleation $k_+^*$, the rate of elongation $k_+$, and the rate of inactivation $k_+^u$.

The rates of nucleation are $(1.0 \pm 0.2) \times 10^{-8}$ L$^3$ g$^{-3}$ min$^{-1}$ for 13 mM ionic strength and $(4.2 \pm 0.5) \times 10^{-4}$ L g$^{-1}$ min$^{-1}$ for the other ionic strengths. Figure 3 shows the values of the rate of elongation plotted as a function of the ionic strength of the solution. One can see that the rate of fibril elongation increases with increasing ionic strength. Knowing the rate of nucleation and the rate of elongation, we can estimate the rate of inactivation $k_+^u$ by using Eq. (16). It is $(1.5 \pm 0.5) \times 10^{-2}$ min$^{-1}$ for 13 mM ionic strength and about $0.3 \pm 0.1$ min$^{-1}$ for the other ionic strengths. The outcome of the aggregation is determined by the balance between the rate of nucleation and the rate of elongation. At low ionic strength the rate of nucleation is very low, the elongation dominates the process of aggregation and, as a result, we obtain very long fibrils.[1,2] At higher ionic strengths, the rate of nucleation strongly increases and as a result, the obtained fibrils are shorter.[2] The increased rate of elongation is also responsible for the decrease in the critical concentration, because the rate of inactivation levels off at higher ionic strength.

The rates of denaturation and aggregation of $\beta$-lg at different conditions have been extensively studied.[6,7,15] In most of the studies, however, the denaturation and the aggregation cannot be separated from each other, especially when a kinetic model, based on one rate-determining reaction, is used. Such an approach bears the risk of overestimating the order

of the denaturation reaction and underestimating the order of the aggregation reaction. Moreover, fitting of experimental data with one model equation and determining of the order of the kinetics judging by the quality of the fit is not always justified. Jaskulka *et al.*,[10] following a rigorous statistical approach, showed for a number of kinetic studies that in many cases the criterion for the quality of the fit used in the study was misleading. Physically, finding the order of a denaturation reaction to be greater than unity means that one considers denaturation together with aggregation. Alternatively, our approach explicitly separates the aggregation and the (irreversible) denaturation, the inactivation step in our model, by using different rate constants in the system (10)–(14) and allows the determination of a quantitative estimate of the rate constants of the model (see Fig. 3). We have to also point out that in heat-induced $\beta$-lg aggregation the inactivation step in our model is not observed at *p*H 7.0 and is specific to *p*H 2.0, whereas the activation step, i.e., the protein unfolding, that we have not included in our model, is not *p*H specific.

By combining a relevant kinetic model with experimental results from a sensitive *in situ* technique we are able to elucidate the reaction mechanism of the fibrilar aggregation of $\beta$-lg in considerable detail. A full description of the process, however, can be achieved only by using an experimental method that allows quantitative kinetic data not only in the early stages of aggregation but also in later stages of the process. Such a technique should be combined with a numerical solution of the full kinetic model (2). One suitable method is the proton NMR spectroscopy that we have used in our previous work.[1] Naturally, in the case of $\beta$-lg at *p*H 2.0, at longer heating times the aggregation leads to gelling of the solution which further complicates the description of the dynamics of the system. Another experimental method that can yield more information for the kinetics of $\beta$-lg aggregation is time-resolved small-angle neutron scattering (SANS).[16–18]

## CONCLUSIONS

We have derived a kinetic model for the heat-induced aggregation of $\beta$-lg at *p*H 2.0. The model describes very well the experimental data obtained by *in situ* light scattering. In particular, it explains the existence of an apparent critical concentration for fibril formation in a quantitative way. It also allows us to obtain molecular parameters for the kinetics of fibrilar aggregation of $\beta$-lg as a function of the ionic strength. We obtain the size of the critical nucleus for the fibril formation and the rates in the kinetic equations as a function of the ionic strength. In the case of a 13 mM ionic strength, the critical nucleus consists of approximately four monomers; for all the other ionic strengths studied it is a dimer. This shows the important role that the nonspecific electrostatic interaction plays for the fibrilar aggregation of $\beta$-lg at *p*H 2.0. The electrostatic interaction strongly affects the rate of nucleation and elongation: the higher the ionic strength, the faster the nucleation and elongation.

## ACKNOWLEDGMENTS

This work was supported by the Netherlands Research Council for Chemical Sciences (CW) with financial aid from the Netherlands Organization for Scientific Research (NWO), in the context of the SOFTLINK program "Theoretical Biophysics of Proteins in Complex Fluids."

## APPENDIX: ANALYTICAL SOLUTION OF THE KINETIC MODEL

To find the solution of the set (10)–(14) we introduce the following dimensionless variables and parameters:

$$x = c_1^b/c_0, \quad y = c_p/c_0, \quad z = c_h/c_0, \quad f = c_d/c_0,$$
$$\tau = k_+^u t, \quad a = \frac{k_+^* c_0^{n^*-1}}{k_+^u}, \quad b = \frac{k_+ c_0}{k_+^u}. \tag{A1}$$

Then the set (10)–(14) becomes

$$\frac{dx(\tau)}{d\tau} = 1 - [x(\tau) + z(\tau)], \tag{A2}$$

$$\frac{dy(\tau)}{d\tau} = a - an^*[x(\tau) + z(\tau)], \tag{A3}$$

$$\frac{dz(\tau)}{d\tau} = n^* \frac{dy(\tau)}{d\tau} + by(\tau), \tag{A4}$$

$$\frac{df(\tau)}{d\tau} = (n^*)^2 \frac{dy(\tau)}{d\tau} + by(\tau) + 2bz(\tau), \tag{A5}$$

with the corresponding initial conditions,

$$x(0) = 0, \quad y(0) = 0, \quad z(0) = 0, \quad f(0) = 0. \tag{A6}$$

The set (A2)–(A6) has an analytical solution which can be written in the form

$$x(\tau) = \frac{n^* - 1}{n^*}\tau + \frac{1}{\beta n^*}\exp(-\beta\tau)\frac{\sinh(\beta\tau\sqrt{1-\chi})}{\sqrt{1-\chi}} + \frac{(1-n^*)}{ab(n^*)^2}\left\{1 - \exp(-\beta\tau)\left[\frac{\sinh(\beta\tau\sqrt{1-\chi})}{\sqrt{1-\chi}} + \cosh(\beta\tau\sqrt{1-\chi})\right]\right\}, \tag{A7}$$

$$y(\tau) = \frac{a}{\beta}\exp(-\beta\tau)\frac{\sinh(\beta\tau\sqrt{1-\chi})}{\sqrt{1-\chi}} - \frac{n^* - 1}{bn^*}\left\{1 - \exp(-\beta\tau)\left[\frac{\sinh(\beta\tau\sqrt{1-\chi})}{\sqrt{1-\chi}} + \cosh(\beta\tau\sqrt{1-\chi})\right]\right\}, \tag{A8}$$

$$z(\tau) = \left[\frac{1}{n^*} - \frac{n^*(n^*-1)}{\beta^2\chi} + \frac{2(n^*-1)}{n^*\beta\chi}\right]\left\{1 - \exp(-\beta\tau)\left[\frac{\sinh(\beta\tau\sqrt{1-\chi})}{\sqrt{1-\chi}} + \cosh(\beta\tau\sqrt{1-\chi})\right]\right\} - \frac{n^*-1}{n^*}\tau + \frac{2\beta - n^*}{\beta n^*}\exp(-\beta\tau)\frac{\sinh(\beta\tau\sqrt{1-\chi})}{\sqrt{1-\chi}}, \tag{A9}$$

$$f(\tau) = \left\{\frac{1}{n^*} + 2 - \frac{n^*(n^*-1)}{\beta^2\chi} + \frac{2}{\beta\chi}\left[2n^* - 1 - \frac{2b+1}{n^*}\right] - \frac{2b(n^*-1)(4-\chi)}{n^*\beta^2\chi^2}\right\}[1 - \exp(-\beta\tau)\cosh(\beta\tau\sqrt{1-\chi})] + \left\{2 - \frac{1}{\beta} - \frac{2-\chi}{\beta\chi}\left[2n^* - 1 - \frac{2b+1}{n^*}\right] - \frac{2b(n^*-1)(3\chi-4)}{n^*\beta^2\chi^2}\right\}\exp(-\beta\tau)\frac{\sinh(\beta\tau\sqrt{1-\chi})}{\sqrt{1-\chi}} - \left[2n^* - 1 - \frac{2b+1}{n^*} - \frac{4b(n^*-1)}{n^*\beta\chi}\right]\tau + \frac{b(n^*-1)}{n^*}\tau^2. \tag{A10}$$


[1] L. N. Arnaudov, R. de Vries, H. Ippel, and C. P. M. van Mierlo, Biomacromolecules **4**, 1614 (2003).
[2] L. N. Arnaudov and R. de Vries, Biomacromolecules **7**, 3490 (2006).
[3] F. Oosawa and S. Asakura, *Thermodynamics of Polymerization of Protein* (Academic, New York, 1975).
[4] J. H. Come, P. E. Fraser, and P. T. Lansbury, Proc. Natl. Acad. Sci. U.S.A. **90**, 5959 (1993).
[5] S. P. F. M. Roefs and K. G. de Kruif, Eur. J. Biochem. **226**, 883 (1994).
[6] M. A. M. Hoffmann, S. P. F. M. Roefs, M. Verheul, P. J. J. M. van Mil, and K. G. de Kruif, J. Dairy Res. **63**, 423 (1996).
[7] M. Verheul, S. P. F. M. Roefs, and K. G. de Kruif, J. Agric. Food Chem. **46**, 896 (1998).
[8] A. Lomakin, D. S. Chung, G. B. Benedek, D. A. Kirschner, and D. B. Teplow, Proc. Natl. Acad. Sci. U.S.A. **93**, 1125 (1996).
[9] A. Lomakin, D. B. Teplow, D. A. Kirschner, and G. Benedek, Proc. Natl. Acad. Sci. U.S.A. **94**, 7942 (1997).
[10] F. J. Jaskulka, D. E. Smith, and K. Larntz, Int. Dairy J. **10**, 589 (2000).
[11] F. Ferrone, Methods Enzymol. **309**, 256 (1999).
[12] V. P. Zhdanov and B. Kasemo, Langmuir **20**, 2443 (2004).
[13] B. Vollmert, *Polymer Chemistry* (Springer, Berlin, 1973).
[14] H. C. Van de Hulst, *Light Scattering by Small Particles* (Dover, New York, 1981).
[15] Le C. Bon, T. Nicolai and D. Durand, Macromolecules **32**, 6120 (1999).
[16] P. Aymard, T. Nicolai and D. Durand, Macromolecules **32**, 2542 (1999).
[17] M. Verheul, J. S. Pedersen, S. P. F. M. Roefs, and K. G. de Kruif, Biopolymers **49**, 11 (1999).
[18] L. N. Arnaudov, R. de Vries, and M. A. Cohen Stuart, J. Chem. Phys. **124**, 084701 (2006).